Journal of Statistical Physics, Vol. 107, Nos. 1/2, April 2002 (© 2002)

Mesoscopic Simulation of Polymers in Fluid Dynamics Problems

S. M. Willemsen,[1] H. C. J. Hoefsloot,[1] and P. D. Iedema[1]

Received February 1, 2001; accepted October 22, 2001

Dissipative Particle Dynamics has been used effectively as a modelling technique to perform Computational Fluid Dynamics. DPD preserves some molecular detail whereas in classical CFD this is lost. The technique has been tested in two cases of macromolecules in flow simulations. First, the behaviour of a polymer within a square capillary has been studied, which is the basis of hydrodynamic chromatography. Secondly, the effect of polymers on the melting in shear flow has been simulated.

KEY WORDS: Dissipative Particle Dynamics; Computational Fluid Dynamics; phase change; chromatography; polymers.

1. INTRODUCTION

Dissipative Particle Dynamics[1] can be best described as a type of coarse grained Molecular Dynamics. The particles in DPD are not single molecules but represent a mesoscopic cluster of molecules. The method has shown to be a very flexible tool especially for complex fluid simulations. It has been used in a wide variety of areas[2] such as suspensions,[3] multicomponent flows,[4] phase separation in polymer systems,[5] and thermal problems.[6, 7]

In DPD particles experience interaction forces from particles in their proximity. The interaction is pairwise and total momentum is conserved. It has been shown both theoretically[8] and by simulation[9] that the macroscopic behaviour is hydrodynamical. Since the interactions have a stochastic component, Brownian motion can be taken into account.

[1] Department of Chemical Engineering, University of Amsterdam, Nieuwe Achtergracht 166, 1018 WV Amsterdam, The Netherlands; e-mail: piet@science.uva.nl

0022-4715/02/0400-0053/0 © 2002 Plenum Publishing Corporation

As a shortcoming in DPD the total energy is not conserved, but this problem has been solved recently by both Avalos and Mackie[10] and Español.[11] An other deficiency arises in the modelling of solid walls. When modelling the solid as particles with zero velocity a no slip condition at the wall could only be achieved by increasing the density of particles in the wall resulting in a low density region near the wall. A method to solve these problems is described in Willemsen *et al.*[9]

As one of the merits of DPD polymers can be simulated very easily, by attaching springs between particles. This just adds an extra spring force between the two attached particles. This concept has been shown to adequately describe both thermodynamic[5] and fluid flow behaviour of polymeric liquids.[12] The beauty of the method lies in its preserving of some molecular detail while simulating macroscopic flow. This means that along with the position of the polymer the orientation and radius of gyration can be calculated. The scaling laws that emerge for these DPD polymers are in good agreement with well established theory.[12, 13]

In this article the advantages of incorporating polymers in a DPD simulation will be exploited. We will show that DPD is a powerful tool when studying the behaviour of polymers in a flow field. In order to do so two systems are considered. The first describes the behaviour of polymers of different sizes flowing in a narrow channel. In the other a solid polymer particle is melted in shear flow. In both cases the coordinates of the beads of the polymer are known so the behaviour of the polymer can be studied with a resolution down to the molecular shape.

In the case of flow through a narrow channel the mean velocity of the polymer will differ from the mean velocity of the solute. This is due to the difference in size of the solute and a polymer molecule. The larger the polymer molecule the more difficult it is for the centre of mass of this molecule to be close to the wall. Therefore the polymer will not be subjected to the low velocities in the vicinity of the wall and hence on average have a larger velocity than a solute molecule. A macromolecule separation technique called hydrodynamic chromatography is based on this principle.

In the case of melting in a shear flow the solid consists either of single DPD particles or of a number of strings of particles (polymer). In this way the effect of the solid consisting of a polymer can be studied while all other properties are kept constant. The difference between the systems becomes clear at the very instant the individual particles (either or not in a chain) reach the melting temperature. A single particle becomes mobile and can move away from the solid instantaneously. In contrast, the mobility of a particle of a chain is co-determined by the conditions of the other particles in the chain.

The remainder of this paper is organised as follows. First the model is explained. Then the two cases: hydrodynamics chromatography and melting in shear flow, a problem description, computational details and results are presented. Finally in the last section some conclusions are drawn.

2. THE DPD MODEL

2.1. Classical DPD

For completeness the DPD scheme will be given, although it can be found in many places in literature. The time evolution of the positions ($\mathbf{r}_i(t)$) and impulses ($\mathbf{p}_i(t)$) (for simplicity we take the masses of all particles 1) of the imaginary particle is given by:

$$\frac{d\mathbf{r}_i}{dt} = \mathbf{v}_i(t), \qquad \frac{d\mathbf{v}_i}{dt} = \mathbf{f}_i(t) \tag{1}$$

The force acting on the particles can be seen as a combination of three parts:

$$\mathbf{f}_i(t) = \sum_{j \neq i} (\mathbf{F}_{ij}^C + \mathbf{F}_{ij}^D + \mathbf{F}_{ij}^R) \tag{2}$$

The first part is the conservative force

$$\mathbf{F}_{ij}^C = \begin{cases} a_{ij}\left(1 - \dfrac{r_{ij}}{r_c}\right)\hat{\mathbf{r}}_{ij} & (r_{ij} < r_c) \\ 0 & (r_{ij} \geqslant r_c) \end{cases} \tag{3}$$

where a_{ij} is the maximum repulsion between particle i and j, $\mathbf{r}_{ij} = \mathbf{r}_i - \mathbf{r}_j$, $r_{ij} = |\mathbf{r}_{ij}|$, $\hat{\mathbf{r}}_{ij} = \mathbf{r}_{ij}/|\mathbf{r}_{ij}|$, and r_c is the cut-off radius. The second and third force are the dissipative and the random force:

$$\begin{aligned} \mathbf{F}_{ij}^D &= -\gamma\omega^D(r_{ij})(\hat{\mathbf{r}}_{ij} \cdot \mathbf{v}_{ij})\,\hat{\mathbf{r}}_{ij} \\ \mathbf{F}_{ij}^R &= \sigma\omega^R(r_{ij})\,\theta_{ij}\hat{\mathbf{r}}_{ij} \end{aligned} \tag{4}$$

In which $\mathbf{v}_{ij} = \mathbf{v}_i - \mathbf{v}_j$, γ is the friction coefficient and σ is the noise amplitude, $\omega(r_{ij})$ is a weight function, which tends to zero for $r = r_c$, and θ_{ij} is a random number from a Gaussian distribution with zero mean and $1/dt$ variance.

Espagñol and Warren[8] showed that the weight functions and constants in these forces can be chosen arbitrarily, but they should obey:

$$\begin{aligned}[\omega^R(r_{ij})]^2 &= \omega^D(r_{ij}) \\ \sigma^2 &= 2k_B T\gamma\end{aligned} \tag{5}$$

with k_B the Boltzmann constant, which is the unit of energy.

The equations of motion are solved using the modified velocity-Verlet algorithm as presented by Groot and Warren.[5] The weight function for the random force has the following functional form: $\omega^R(r_{ij}) = 1 - \frac{r}{r_c}$, and we choose $r_c = 1.0$, which is the unit of length.

2.2. Energy Conserving DPD

When energy conservation plays an important role, as in our melting simulations, two extra variables need to be considered: the internal energy and the temperature. Since the temperature of the individual DPD particles may vary, it is no longer possible to use Eq. (5) to calculate the friction coefficient γ and the noise amplitude σ. However, Español[11] suggests to keep the noise amplitude constant for all particles and to determine the friction constant from the fluctuating temperatures:

$$\gamma_{ij} = \frac{\sigma^2}{4}\left[\frac{1}{T_i} + \frac{1}{T_j}\right] \tag{6}$$

where T_i is the temperature of particle i. The evolution of the internal energy ϵ_i is given by:

$$\begin{aligned}\frac{d\epsilon_i}{dt} = \frac{1}{2}\Bigg[&\sum_j \left[\omega_D(r_{ij})\,\gamma_{ij}(\mathbf{v}_{ij}\cdot\hat{r}_{ij})^2 - \sigma_{ij}^2\omega_R^2(r_{ij})\right] - \sum_j \sigma_{ij}\omega_R(r_{ij})(\mathbf{v}_{ij}\cdot\hat{r}_{ij})\,\theta_{ij}^V \Bigg] \\ &+ \sum_j \kappa_{ij}\left(\frac{1}{T_i} - \frac{1}{T_j}\right)\omega_{TD}(r_{ij}) + \sum_j \alpha_{ij}\omega_{TR}(r_{ij})\,\theta_{ij}^T\end{aligned} \tag{7}$$

θ_{ij}^V and θ_{ij}^T are uncorrelated random numbers from a Gaussian distribution with zero mean and $1/dt$ variance.

The upper part of this equation is related to viscous heating of the particles, while the lower part is related to the conduction of heat. κ_{ij} represents a thermal conductivity, that depends on the internal energy of particles i and j and follows from[11]:

$$\kappa_{ij} = \frac{\tilde{\kappa}}{\lambda^2}\frac{T_i + T_j}{2}\frac{\epsilon_i + \epsilon_j}{2} \tag{8}$$

Here, λ is the average distance between particles and $\tilde{\kappa}$ is the thermal diffusivity.

Finally, the detailed balance condition requires that $\alpha_{ij}^2 = 2\kappa_{ij}$, and the following relationship between the weight functions[8]:

$$\begin{aligned} \omega_R^2(r_{ij}) &= \omega_D(r_{ij}) \\ \omega_{TR}^2(r_{ij}) &= \omega_{TD}(r_{ij}) \end{aligned} \tag{9}$$

This just leaves the relation between the internal energy and the temperature of the DPD particles. In the case of a material that changes phase three stages can be defined. First the material is solid (with a solid heat capacity), then the solid will melt, and finally the material is completely liquid (with a liquid heat capacity). This leads to the following equation of state:

$$T(\epsilon) = \begin{cases} \dfrac{\epsilon}{C_{v,s}} & \epsilon < T_m \cdot C_{v,s} \\ T_m & T_m \cdot C_{v,s} \leqslant \epsilon \leqslant T_m \cdot C_{v,s} + L \\ T_m + \dfrac{\epsilon - L - T_m \cdot C_{v,s}}{C_{v,l}} & \epsilon > T_m \cdot C_{v,s} + L \end{cases} \tag{10}$$

where $C_{v,s}$ and $C_{v,l}$ are the solid and liquid heat capacities, T_m is the melting temperature and L is the enthalpy of fusion. This equation of state is similar to the enthalpy method[14] commonly used in phase change problems.

3. HYDRODYNAMIC CHROMATOGRAPHY

3.1. Problem Description

Pressure driven flow through a rectangular pipe is a problem that is interesting for chromatography as shown by Cifuentes and Poppe.[15] We want to study the principles of a chromatographical method called hydrodynamic chromatography. Macromolecules are separated according to their difference in size. This is realised in capillaries of small sizes even on chip like devices.[16] The lateral dimensions of the capillary are only between one and three orders of magnitude larger than the dimensions of the polymer. This circumstance enables us to perform a DPD simulation of the macroscopic flow together with a polymer. The system under consideration in this paper is a square pipe where the driving force for the flow is a pressure drop.

3.2. Computational Detail

Simulations are performed in a $8 \times 8 \times 8$ sized simulation box containing 5120 particles. The z-direction is the direction of flow, solid walls are created at both sides (x-direction) and top and bottom (y-direction) on which a no-slip boundary condition is imposed as described by Willemsen *et al.*[9] Because we want to simulate a very long capillary a periodic boundary is created in the z-direction. The first problem is to check whether the box in z-direction is large enough in order to have no effect from the polymer molecule on itself. By performing simulations with different sizes it turned out that $8r_c$ in the z-direction is sufficient for polymers up to length 20.

The second problem is how to deal with the pressure gradient. Applying standard DPD with a periodic boundary condition would not lead to the desired result of a constant pressure drop but it would give a saw-tooth pressure profile. Because the pressure drop over the pipe is constant it can be treated as being simply a body force in the z-direction. So in the momentum balance for every DPD particle a force in the z-direction is added. The value of this force is 0.005.

As has been pointed out by Groot and Warren[5] the difference in maximal repulsion between two different species (e.g., $a_{AB} - a_{AA}$) is proportional to the Flory–Huggings χ parameter. This is a measure of the polymer's solubility in the solute: if $\chi = 0$ the polymer would be perfectly soluble, a larger χ stands for a worse solubility. Since the solubility influences the radius of gyration this is an important parameter to describe the separation. We have chosen the parameters for polymer–polymer and monomer–monomer interaction to be $a_{ii} = 3.0$ and the polymer–monomer interaction to be $a_{ij} = 4.0$.

The temperature of the simulations is chosen to be $k_B T = 0.1$, $\sigma = 10.0$ and the timestep is 0.01. The system was equilibrated for 10^4 timesteps after which the simulation ran for $5 \cdot 10^5$ steps.

3.3. Results

Before studying the flow of solute plus polymer, the flow of solute only is analyzed. Therefore the axial velocities are averaged in space over a 29×29 (x, y) grid, and in $5 \cdot 10^5$ steps over time. In the article of Cifuentes and Poppe[15] an analytical solution is given for this flow. It reads:

$$V_z(x, y) = \frac{1 - x^2}{2} - 16 \sum_{j=1,3,5\ldots}^{\infty} (-1)^{\frac{j-1}{2}} \frac{\cos(\frac{j\pi x}{2}) \cosh(\frac{j\pi y}{2}) \operatorname{sech}(\frac{j\pi \phi}{2})}{(j\pi)^3} \tag{11}$$

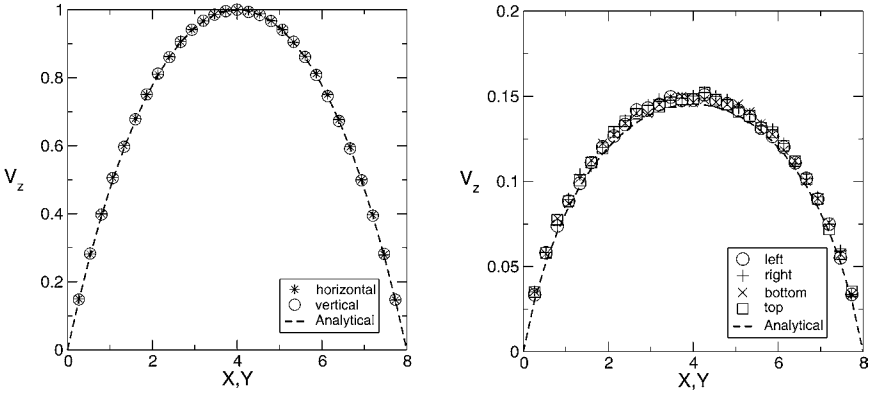

(a) centre X,Y = 4.0 (b) wall X, Y = 0.27

Fig. 1. Comparison of the averaged axial velocity from the DPD simulation and the analytical solution at different position in the capillary. In the left picture the velocity profile in the centre of the capillary is is plotted. In the right picture the velocity profile close to the four walls of the capillary (designated left,right,top and bottom) are shown. The simulation results are normalised with the maximal velocity ($V_{z,\max} = 0.147$).

where (0, 0) is the middle of the pipe, and the x-coordinate is normalised to run between $[-1, 1]$, and the y-coordinate between $[-\phi, \phi]$. In Fig. 1 the results are depicted for the simulation together with the analytical solution. As can be seen from the graphs the simulation results agree well with the analytical solution.

Now having demonstrated that the flow inside the rectangular pipe can be calculated accurately with DPD, polymer is added. During this simulation the position of the centre of mass of the polymer is determined, and the axial velocity is monitored. Initially the polymer is placed in the middle of the pipe. For the sake of comparison also the movement of a single DPD particle is analyzed. In Fig. 2 the movement of this centre of mass can been followed during a simulation of $2.5 \cdot 10^6$ timesteps. The DPD simulation predicts that the larger polymer remains more distant from the wall than the smaller polymer. Also, the monomer can move up to or even collide with the wall.

In Table I the radius of gyration and the mean velocity of the polymers is shown. It is apparent that this restricted movement though the cross-section of the pipe does influence the mean axial velocity. A general trend is the longer the polymer chain the larger the mean velocity. The discrepancy in this reasoning is the polymer of length 10. However, from Fig. 2 we can see that this is probably due to the method of sampling. This polymer seems to stay in the lower right corner of the capillary for a long time, reducing the mean axial velocity.

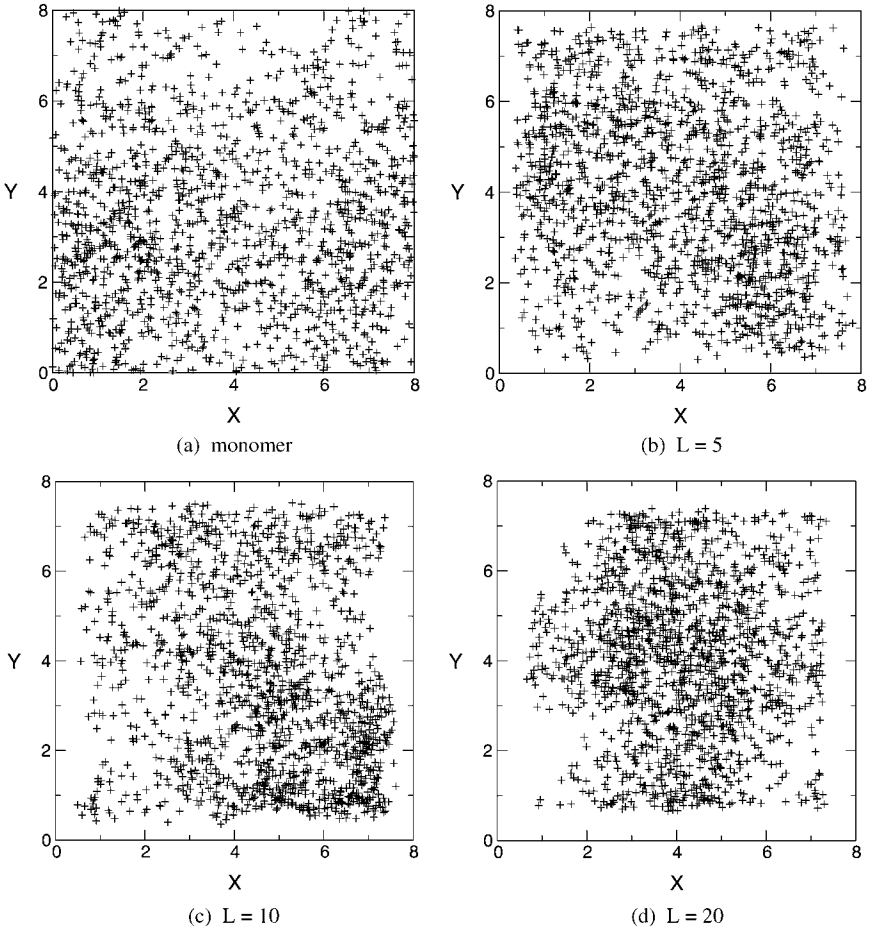

Fig. 2. Position of the centre of mass in the cross-section of the pipe during the simulation for different polymer lengths.

Table I. Radius of Gyration and Mean Velocity for Different Polymer Lengths

Length	Radius of gyration	Mean axial velocity
1	—	0.117
5	0.239	0.138
10	0.409	0.135
20	0.549	0.163

In conclusion, apart from accurately calculating the flow through pipes similar to standard CFD simulations, the incorporation of polymers in DPD indeed enables us to study the behaviour of polymers in these flows. It is demonstrated that the observed behaviour of the polymer chains in such flows is qualitatively well predicted by the DPD simulations.

4. MELTING IN SHEAR FLOW

4.1. Problem Description

Melting of polymeric materials is an important step in polymer processing. Since this mainly takes place in large scale extruders, the dimension of these machines is beyond the reach of DPD. However, the interaction between flow and the melting process can be studied on a smaller scale, giving insight in the specific behaviour of macromolecular materials as compared to non-polymeric materials. We have already shown[7] that it is possible to describe the movement of a melting front in a solid within the DPD framework. In this reference only the change of internal energy was calculated, while the particles were not allowed to move. Here we apply this method to the melting of a solid particle in a flow field. The system to be considered consists of two plates moving in opposite directions, causing shear flow between them. The plates have an elevated temperature (above the melting point of this material). Then a cold particle (below the melting point) is placed between these plates. The particle may consist of monomeric DPD particles or polymeric ones. The difference in melting behaviour has been studied.

4.2. Computational Detail

In these simulations two phases exist. A fluid phase, which has a temperature above the melting point, and a solid phase, which has a temperature equal to or below the melting point. The interaction between the solid and the liquid has been treated in the following way: first the update in energy is calculated [Eq. (7)]. With this updated energy value the new temperature is calculated using the equation of state [Eq. (10)]. Only if the new temperature of the particle is above the melting temperature an update in the velocity and position is calculated. This means that the particles remain at their fixed position and keep a zero velocity as long as they stay below the melting temperature.

The first step in the melting simulations is the creation of the solid. To this end a simulation is performed in a $4 \times 4 \times 4$ (x, y, z) sized simulation box containing 640 particles. The particles put in the simulation box are

either non-connected particles or polymers. This system is allowed to equilibrate for 10^4 timesteps. At the end of this equilibration simulation the particles are shifted to the middle of a $12 \times 24 \times 4$ sized simulation box and given a temperature of 0.029, which is below the melting temperature ($T_m = 0.0295$). Then particles are placed in the remainder of this larger box so that a total of 11520 particles is reached. These new particles are given an initial temperature of 0.030.

At $x = 0$ and $x = 12$ solid walls are present which moving with velocities of $V_y = 1.0$ and $V_y = -1.0$ respectively. Again these walls are modelled as no-slip boundaries. In the other two directions periodic boundaries are used. The walls have a temperature of 0.030.

Further simulation parameters are: $\sigma = 1.0$, thermal conductivity $\tilde{\kappa} = 0.1$, solid and liquid heat capacity $C_{v,s} = C_{v,l} = 10^5$, heat of fusion $L = 500$, the repulsion between all particle monomers or polymers $a_{ii} = a_{ij} = 3.0$, and the timestep is 0.01.

4.3. Results

In Fig. 3 two snapshots of the velocity vectors and the temperature profiles are shown. In the first picture, the conduction of heat in the solid can be seen. Also the formation of two circulation loops, one above and one under the solid is visible. Because of this reversal of flow the solid melts faster on bottom left and top right corners, causing an elliptical shape to form in the later stages of the melting process, as shown in the second picture. Mind that this is not due to a rotation of some sort (since the solid is kept stationary at all times), but merely caused by the asymetry in the melting process in itself.

The melting process can also be studied by monitoring the lowest temperature in the simulation, which typically is the centre temperature of the solid. A graph of this lowest temperature is given in Fig. 4. In the first part of the graph the heating of the solid (through conduction) can be seen. At the instant when the solid reaches the melting temperature (0.0295) its temperature remains constant until the whole solid is molten. Finally it rises to reach the temperature of the walls (0.030). The second line in the graph represents the case when the solid is made of polymer chains of length 10. The heating of the solid (the first part of the graph) is not affected by the construction of the solid. However, it can be seen that the total melting time (this is the time at which the minimal temperature is above the melting temperature) is affected. It takes about 6 persent longer for the polymeric solid to melt. This can be explained as follows: when a DPD particle has reached a temperature above the melting point it can start moving. The bulk flow will take up this particle and move it away

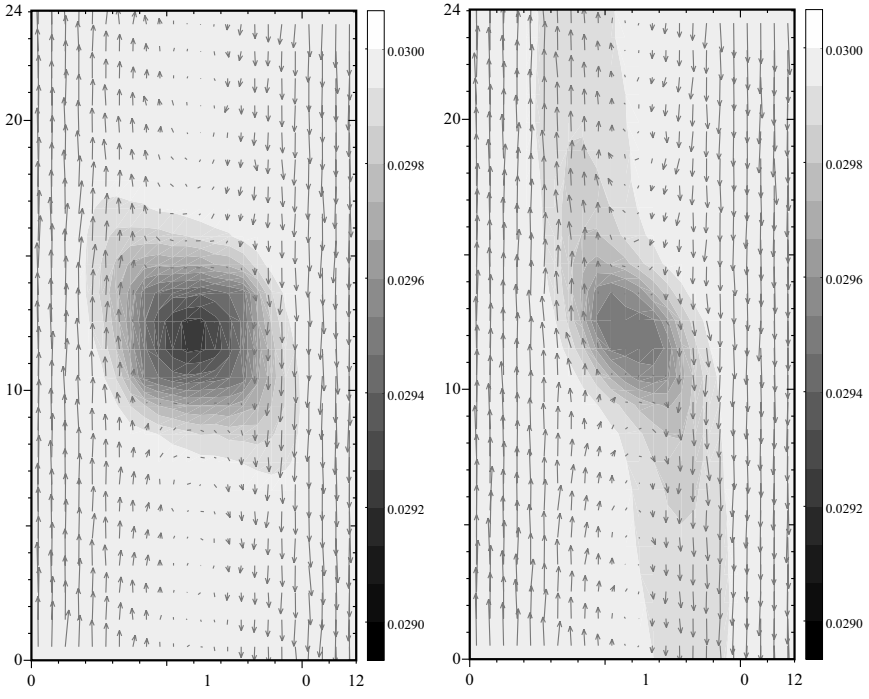

Fig. 3. Two snapshots of the temperature profile and velocity vectors between the two moving plates. The horizontal direction (between 0 and 12) is the x-direction, while vertically (between 0 and 24) the y-direction is plotted. The color bar represents the temperature range. At time = 120 the solid is completely at the melting temperature.

from the solid. However, if this particle is part of a polymer chain, some part of this chain might still be solid. Therefore, the molten DPD particles will still be attached to the solid, and stay near the solid for a longer time, thus hindering the flow of fresh hot particles. So the heat-flow towards the solid will be slower, resulting is a longer total melting time.

This shows that DPD allows the incorporation of molecular effects in a melting simulation, which is not possible in an equally convenient way in conventional CFD. This again demonstrates the benefits of DPD over conventional CFD in problems involving polymers.

5. CONCLUSIONS

In this paper we have demonstrated the benefits of Dissipative Particle Dynamics as a method to solve complex flow problems involving polymers.

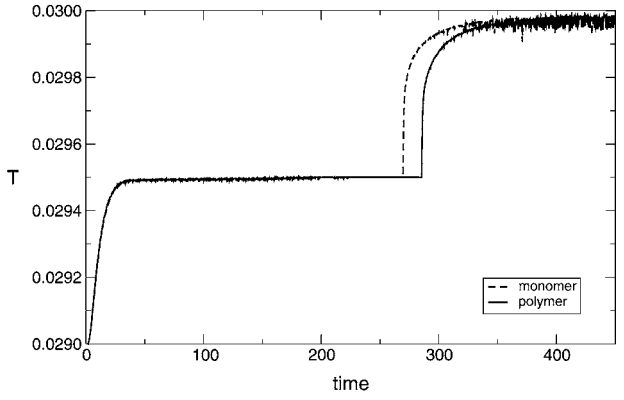

Fig. 4. The minimal temperature occurring in the simulation plotted against simulation time. The dotted line represents the solid created by separate DPD particles, while the solid line represents the solid created by polymer chains of length 10.

First, DPD was tested by comparing the predicted velocity profile for pressure driven flow within a square pipe with an analytical solution. The agreement between the two was found to be good. However, the DPD method has some additional merits, since it is easy to incorporate polymers, which is impossible in the classical CFD framework.

These benefits of DPD have been shown in two case studies. First, the separation principle of hydrodynamic chromatography has been investigated, and observed trends were predicted well by the DPD method. Secondly, the effect of polymer chains on the melting in shear flow has been studied, and the melting of polymers turned out to be slower than of solids constructed of non-connected DPD particles.

The next step in this research is to get quantitative results from the DPD simulations. This requires mapping of DPD parameters. For the case of hydrodynamic chromatography the χ parameter has to be mapped with the repulsion difference between the polymer and the solvent. Furthermore, the ratio between diffusion coefficient and viscosity has to be matched with experimental conditions. For the case of melting, the ratio between heat diffusion and convection has to be matched with experimental conditions.

ACKNOWLEDGMENTS

The authors wish to thank R. Tijssen for discussions on hydrodynamic chromatography, R. E. van Vliet for discussions on the equilibration of the solid, and DSM Research (Geleen, the Netherlands) for financial support.

REFERENCES

1. P. J. Hoogerbrugge and J. M. V. A. Koelman, Simulating microscopic hydrodynamics phenomena with Dissipative Particle Dynamics, *Europhys. Lett.* **19**(3):155–160 (1992).
2. P. B. Warren, Dissipative particle dynamics, *Current Opinion in Colloid & Interface Science* **3**(6):620–624 (1998).
3. J. M. V. A. Koelman and P. J. Hoogerbrugge, Dynamic simulation of hard-sphere suspensions under steady shear, *Europhys. Lett.* **21**(3):363–368 (1993).
4. P. V. Coveney and P. Español, Dissipative Particle Dynamics for interacting multicomponent systems, *J. Phys. A: Math. Gen.* **30**(3):779–784 (1997).
5. R. D. Groot and P. B. Warren, Dissipative Particle Dynamics: Bridging the gap between atomistic and mesoscopic simulation, *J. Chem. Phys.* **107**(11):4423–4435 (1997).
6. A. D. Mackie, J. Bonet Avalos, and V. Navas, Dissipative Particle Dynamics with energy conservation: Modelling of heat flow, *Phys. Chem. Chem. Phys.* **1**(9):2039–2049 (1999).
7. S. M. Willemsen, H. C. J. Hoefsloot, D. C. Visser, P. J. Hamersma, and P. D. Iedema, Modelling phase change with Dissipative Particle Dynamics using a consistent boundary condition, *J. Comp. Phys.* **162**(2):385–394 (2000).
8. P. Español and P. Warren, Statistical mechanics of Dissipative Particle Dynamics, *Europhys. Lett.* **30**(4):191–196 (1995).
9. S. M. Willemsen, H. C. J. Hoefsloot, and P. D. Iedema, No-slip boundary condition in Dissipative Particle Dynamics, *Int. J. Mod. Phys. C* **11**(5):881–890 (2000).
10. J. Bonet Avalos and A. D. Mackie, Dissipative Particle Dynamics with energy conservation, *Europhys. Lett.* **40**(2):141–146 (1997).
11. P. Español, Dissipative Particle Dynamics with energy conservation, *Europhys. Lett.* **40**(6):631–636 (1997).
12. A. G. Schlijper, P. J. Hoogerbrugge, and C. W. Manke, Computer simulation of dilute polymer solutions with the Dissipative Particle Dynamics method, *J. Rheo.* **39**(3):567–579 (1995).
13. N. A. Spenley, Scaling laws for polymers in Dissipative Particle Dynamics, *Europhys. Lett.* **49**(4):534–540 (2000).
14. V. R. Voller and C. Prakash, A fixed grid numerical modelling methodology for convection-diffusion mushy region phase-change problems, *Int. J. Heat Mass Transfer* **30**(8):1709–1718 (1987).
15. A. Cifuentes and H. Poppe, Rectangular capillary electrophoresis: some theoretical considerations, *Chromatographia* **39**(7):391–404 (1994).
16. R. Tijssen, J. Bos, and M. E. Kreveld, Hydrodynamic chromatography of macromolecules in open microcapillary tubes, *Anal. Chem.* **58**:3036–3044 (1986).